coatings

MDPI

Article

Sulfonated Pentablock Copolymer with Graphene Oxide for Co^{2+} Ions Removal: Efficiency, Interaction Mechanisms and Secondary Reaction Products

Simona Filice [1], Viviana Scuderi [1,*], Massimo Zimbone [2], Sebania Libertino [1], Luana La Piana [1], Roberta Agata Farina [1] and Silvia Scalese [1]

[1] Consiglio Nazionale delle Ricerche, Istituto per la Microelettronica e Microsistemi (CNR-IMM), Ottava Strada n.5, 95121 Catania, Italy; simona.filice@imm.cnr.it (S.F.); sebania.libertino@imm.cnr.it (S.L.); luanalapiana@gmail.com (L.L.P.); roberta.farina@imm.cnr.it (R.A.F.); silvia.scalese@imm.cnr.it (S.S.)

[2] Consiglio Nazionale delle Ricerche, Istituto per la Microelettronica e Microsistemi (CNR-IMM), Via S. Sofia 64, 95123 Catania, Italy; massimo.zimbone@ct.infn.it

* Correspondence: viviana.scuderi@imm.cnr.it

Abstract: In this work, sulfonated pentablock copolymer (s-PBC) and s-PBC mixed with graphene oxide (s-PBC_GO) layers were deposited on polypropylene (PP) fibrous filters and tested as active coatings for the removal of cobalt ions from water using adsorption and filtration processes. Some of the coated filters were treated by UV light irradiation to modify their hydrophilic properties. The filters were characterized, before and after the processes, by energy-dispersive X-ray (EDX) analysis and Fourier transform infrared spectroscopy (FT-IR). The Q_t (mg/g) values, defined as the weight ratio between the removed ions and the coating layer, were evaluated. In the case of adsorption processes, the best results for the removal of Co^{2+} ions were achieved by the s-PBC_GO coating, with a Q_t of 37 mg/g compared to 21 mg/g obtained by the s-PBC. This was ascribed to the presence of GO, which contains more favorable sites able to adsorb positive ions from the solution. Vice versa, for filtration processes, the s-PBC coated filters show similar or slightly better results than the s-PBC_GO coated ones. Such differences can be ascribed to the shorter contact time between the solution and the coating layer in the case of filtration, with respect to adsorption processes, thus reducing the chance for the ions to be adsorbed on the GO layers before passing through the filter. A collateral effect, observed in this study and enhanced in the case of UV-treated coatings, is the release of radical oxysulfur species. The mechanisms involved in this effect are discussed and identified as a consequence of the interaction between the coating layers and metal ions. In order to identify the mechanism of oxysulfur radicals formation and considering a water sample closer to real water, the Co^{2+} ions adsorption experiments were conducted in the presence of a competitive organic contaminant (i.e., methyl orange, MO).

Keywords: sulfonated pentablock copolymer; ions removal; adsorption; filtration

Citation: Filice, S.; Scuderi, V.; Zimbone, M.; Libertino, S.; La Piana, L.; Farina, R.A.; Scalese, S. Sulfonated Pentablock Copolymer with Graphene Oxide for Co^{2+} Ions Removal: Efficiency, Interaction Mechanisms and Secondary Reaction Products. *Coatings* **2023**, *13*, 1715. https://doi.org/10.3390/coatings13101715

Academic Editor: Alexandru Enesca

Received: 28 August 2023
Revised: 20 September 2023
Accepted: 27 September 2023
Published: 29 September 2023

1. Introduction

Today, many works are dedicated to finding new approaches and strategies to purify water. In fact, having access to clean water represents a big problem for humanity. Disinfection, decontamination, water reuse and desalination are the points on which research activity is mainly concentrated.

The aim of this study is to propose an active surface coating layer able to increase the metallic ions removal ability of commercial filters. Heavy and radioactive metal ions, originating from anthropogenic sources or for geological reasons, are accumulated in surface and ground water sources and, beyond specific limits, represent a high toxicity risk for humans since they can enter and bioaccumulate in the human body through the food chain [1,2]. Cobalt is essential for the growth of humans, being a main component

of vitamin B12. However, higher concentrations (more than 1 mg/kg (1 ppm) of the bodyweight) are considered toxic to humans [3,4]. Recently, a higher amount of potentially toxic cobalt was found in the wastewater from several industrial sectors [5]. Different methods for the removal of cobalt from water have been reported [6–8], which often show limitations related to the long time equilibrium, low pH, etc. Thus, alternative methods are highly desired.

Several approaches for the removal of contaminants have been investigated, such as adsorption [9,10], photocatalysis [11–13], separation [14], reverse osmosis [15,16], and the precipitation and ion exchange method [17].

For example, the adsorption method is widely used, being cheap and fast [18]. Different materials have been used as an adsorbent, e.g., carbon-based materials, oxides, clay minerals, resin and others [19–21]. One of the most active options is activated carbon that was also tested for the removal of cobalt (Co(II)) from water [1].

Recently, membrane technology has played an important role in this contest, and polymeric materials are at the basis of the development of water treatment devices. In particular, the development of a new generation of materials is receiving great attention, such as porous organic polymers (POPs) [22]. They have interesting properties: they are robust, flexible, lightweight and the dimensions of the pores and channels can be easily varied. Also, the filtering properties of polymeric membranes can be increased by incorporating different materials within the polymers [23,24]. Typical polymers for membrane filtration include polyacrylonitrile (PAN), polyvinylidene fluoride (PVDF), polyethersulfone (PES) and polysulfone (PSF), whose main disadvantages are membrane fouling, low chlorine resistance, low long-term stability, etc. [25–27]. In this contest, a new sulfonated pentablock copolymer (s-PBC, commercialized as Nexar^{TM}) has really interesting properties. The material produced by Kraton LCC is a symmetric pentablock copolymer comprised of poly(*t*-butyl styrene-*b*-hydrogenated isoprene-*b*-sulfonated styrene-*b*-hydrogenated isoprene-*b*-*t*-butyl styrene) (tBS-HI-SS-HI-tBS). This molecular architecture limits sulfonation to the middle block only. In this way the polymer presents controlled swelling, good mechanical properties and mechanical stability. The hydrogenated isoprene block gives the copolymer additional toughness. Although the properties and possible applications of this polymer are still being studied, it is known that the molecular architecture of this polymer results in some characteristics, such as high hydrophilicity, a negative charge, and an acid character useful for the adsorption of anionic and cationic azo dyes, such as methyl orange and methylene blue, respectively [28]. Furthermore, s-PBC/graphene oxide (GO) nanocomposite membranes, obtained by dispersing GO within a polymer solution, showed good adsorption capabilities, in particular for the removal of different heavy metal ions (Ni^{2+}, Co^{2+}, Cr^{3+} and Pb^{2+}) present at different concentrations in aqueous solutions [29]. Similarly, a photodegradation activity under UV or visible light was observed for composite films obtained by dispersing inorganic semiconductors (i.e., TiO_2 and Bi_2O_3) inside the polymeric layer and these were tested for the photodegradation of dyes [28,30].

Starting from these results, s-PBC (Nexar^{TM}) was recently proposed to be applied as a multifunctional coating for water filters [31–33]. Thanks to its properties (hydrophilicity, acidity, etc.), it was possible to counteract the adhesion and proliferation of *P. aeruginosa planktonica* and *Legionella*. At the same time, the coated filters have shown excellent ability to remove dyes and Fe^{3+} and Co^{2+} ions from aqueous solutions. These abilities depend on the presence of sulphonic groups in the polymeric material, which are directly involved in metal ion adsorption and antibacterial and antibiofouling activity.

In this work, we coated polypropylene (PP) fibrous filters with s-PBC mixed with graphene oxide (s-PBC_GO) in order to have an active surface for the adsorption/filtration of cobalt ions. The PP filter has both the role of support and a porous structure. The s-PBC and s-PBC_GO layers provide useful additional functionalities to the commercial filter for a specific scope. The UV treatment of the coated filters' surface was also investigated to further enhance their performance. The S-PBC filters showed a better removal performance

during the filtration process; on the other hand, the s-PBC_GO filters had a better removal performance during the adsorption process.

As a collateral effect, the formation and release of radical oxysulfur species was observed during the removal processes, and this was enhanced in the case of UV-treated coatings. It is known that water purification treatments are very often responsible for the formation of secondary reaction products, which cannot be reprocessed [34]. For this reason, the interaction between the cobalt ions and the surface of the filters, and the mechanism for the formation of byproducts, were investigated. The filters were characterized before and after use by energy-dispersive X-ray (EDX) analysis and Fourier transform infrared spectroscopy (FT-IR). Finally, considering that in real wastewater different contaminants can occur and interact, affecting the final removal efficiency positively or negatively, Co^{2+} ions adsorption by the coated filters was tested in the presence of an additional competitive contaminant (i.e., MO). The adsorption experiment, performed with the simultaneous presence of the two contaminants, was useful to understand the mechanisms of radical species generation.

2. Materials and Methods

Polypropylene (PP) filters were produced using the melt-blown technology process, as reported in [35]. The fibers have a diameter smaller than 5 µm and create a three-dimensional network. The filter porosity ε_F was 0.98 and was determined by $\varepsilon_F = 1 - \rho_{SF}/(\rho_F \cdot L)$, where r_{SF} is the surface density calculated as the mass of the filter divided by the surface area (m_F/A_F), ρ_F is the fiber's material density (910 Kg/m^3 for polypropylene was used) and L is the PP filter thickness. The coating material was prepared starting from the commercial Nexar solution (10 wt%–12 wt% polymer in a cyclohexane/heptane mixed solvent), with a sulfonation degree of 52 mol% and an ion exchange capacity (IEC) value of 2.0 meq/g [33]. A solution of s-PBC (0.3 g/mL) was prepared by redispersing 3 g of polymer (after commercial solvents evaporation) in 10 mL of a polar solvent (isopropyl alcohol, IPA). A polar solvent is usually preferred for two reasons: the first one is to induce the ion-rich pathway and channels in the casted film, that can facilitate the diffusion of ions and/or other polar species through the nanostructured medium; the second reason concerns the use of an appropriate solvent to obtain the homogeneous dispersion of GO flakes into the polymeric matrix. For this scope, 1 mL of GO (2 mg/mL) was redispersed in the same solvent and added to the polymer solution. The final wt (%) of GO in the polymeric film was 0.67%. The PP filters were cut into circular coupons and coated with the s-PBC (reference) and s-PBC_GO solutions to obtain the PP-modified filters.

A schematic illustration, showing the preparation of the materials, is reported in Figure 1.

For the adsorption and filtration tests, the PP filters have a circular shape with a thickness of ~0.3 cm, and a diameter of ~2.25 and ~5 cm, respectively. Samples were air dried for 24 h before weighing with a precision microbalance. A total of 1 mL of s-PBC/s-PBC_GO solution was deposited (drop casting) on the PP coupons to cover its surface, leading to the amount of deposited layer of $\approx 0.030 \pm 0.001$ g for each coupon. The filters were coated with 5 mL of s-PBC/s-PBC_GO solution and the amount of deposited s-PBC was $\approx 0.147 \pm 0.001$ g for each filter.

Some of the s-PBC@PP and s-PBC_GO@PP samples underwent a UV irradiation process for 7 h, respectively (here named s-PBC@PP_UV and s-PBC_GO@PP_UV). The irradiation was performed by an 18 W UVA/blue DULUX n.78 OSRAM lamp (producing mainly UV emission at 365 nm and a few narrow lines in the visible range).

The surface morphology and the chemical composition of the samples were characterized by a field emission scanning electron microscope (Supra 35 FE-SEM by Zeiss, Oberkochen, Germany), equipped with an energy-dispersive X-ray (EDX) microanalysis system (X-Max, 80 mm^2 by Oxford Instruments, Abingdon, UK). The hydrophilicity of the samples' surface was investigated using the water uptake, in accordance with Equation (1):

$$\text{Uptake\%} = [(m_{wet} - m_{dry})/m_{dry}] \times 100 \quad (1)$$

where m_{dry} is the mass of the sample air dried for at least 24 h and then put into a desiccator, and m_{wet} is the weight of the sample soaked in distilled water at room temperature for 48 h and quickly wiped with a paper tissue in order to remove most of the free surface water.

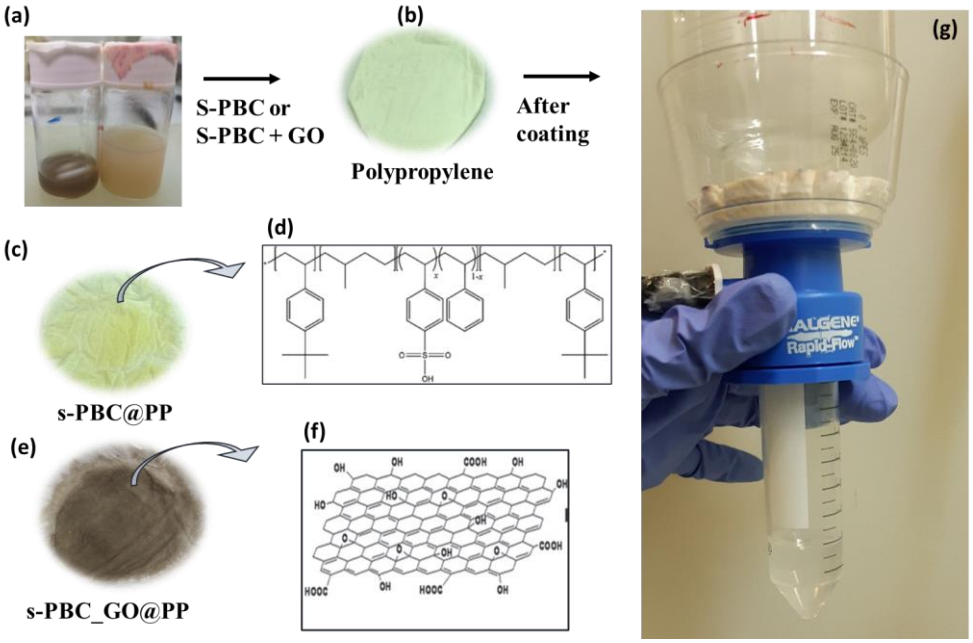

Figure 1. Preparation of s-PBC and s-PBC_GO coated filters. (**a**) Solution of Nexar and Nexar + GO; (**b**) uncoated PP filter; (**c**) PP filter after s-PBC deposition; (**d**) s-PBC structure; (**e**) PP filter after s-PBC_GO deposition; (**f**) GO structure; (**g**) commercial vacuum filtration system (Nalgene®) used for filtration experiment in this work.

At the beginning, the PP surface was hydrophobic and turned hydrophilic after the deposition of the coating layers: the initial PP water uptake was 3% and this increased up to 160% and 230% in the presence of the s-PBC and s-PBC_GO layers, respectively. The UV irradiation resulted in increasing the hydrophilic nature of the s-PBC and s-PBC_GO filters, since the water uptake values increased up to 184% and 270%, respectively.

IR measurements were performed using a Jasco FT/IR-4700 spectrophotometer (JASCO, Tokyo Japan), equipped with an ATR (ATR Pro-one) with a diamond prism.

Adsorption and filtration tests on the Co^{2+} metal ions in water were conducted for all the samples. As a reference, unmodified PP samples were used to highlight the role played by the s-PBC and s-PBC_GO coverage. For the adsorption experiments, the samples were immersed for three hours in the dark in 5 mL of 17.5 mM $CoCl_2$ aqueous solution. This specific concentration was chosen to be able to detect, with sufficient sensitivity, the occurring Co^{2+} concentration changes using UV–Vis absorbance spectroscopy. The initial pH was around neutrality and changes to the lower values occurred instantly (about 2) after membrane immersion, due to the coating acidity.

In the filtration processes, three different 20 mL solutions containing the contaminant were filtered. Each solution was filtered several times, consecutively. The tests were conducted using commercial systems (Nalgene®, Thermo Fisher Scientific, Waltham, Massachusetts, United States), where the PES Supor® machV membrane was removed and replaced with the filters to be tested (Figure 1g). The average flow rate (mL/s) was calculated for all the filters, by filtering 40 mL of H_2O four times. The average values obtained were 4.18, 4.11 and 4.87 mL/s for PP, s-PBC@PP and s-PB@/PP_UV, respectively. For samples with GO, lower flux values were obtained, i.e., 0.43 and 0.25 mL/s for s-PBC_GO@PP and s-PBC_GO@/PP_UV, respectively.

The removal of the contaminant during both the absorption and filtration processes was evaluated through the variation of the absorbance spectra. The spectra were acquired

through an Agilent Cary 50 UV/Vis spectrophotometer (Santa Clara, CA, USA), in a wavelength range between 200 nm and 800 nm. Co^{2+} removal was evaluated by following the evolution of the peak, centered at approximately 527 nm, using the Lambert–Beer law. The formation of secondary species during the absorption and filtration tests was evaluated by recording the absorbance peak at 250 nm.

3. Results and Discussion

Figure 2 reports the FT-IR spectra of the PP (black line), s-PBC@PP (red line) and s-PBC_GO@PP (blue line) samples in the range 4000–500 cm^{-1} (Figure 2a). An enlargement of the region between 1600–500 cm^{-1} is shown in Figure 2b. For the UV-treated samples, no differences were observed in the IR spectra (not shown here).

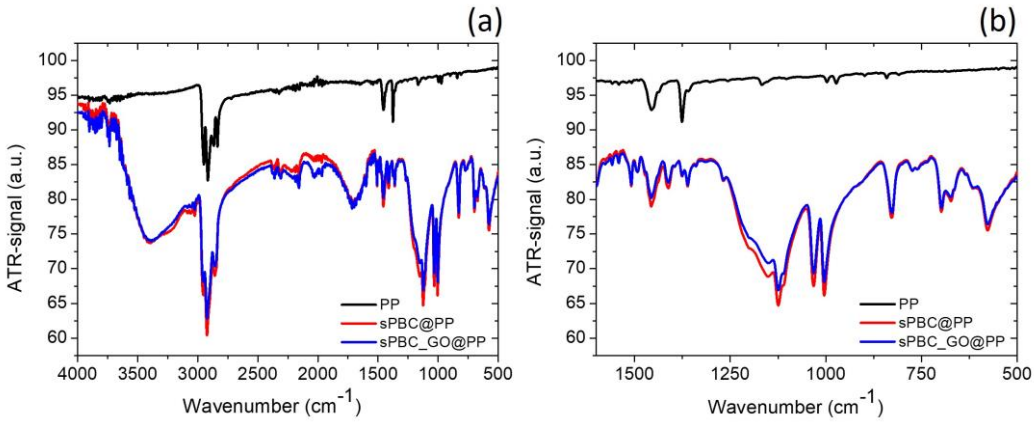

Figure 2. FT-IR spectra of a PP filter (black line), s-PBC@PP filter (red line) and s-PBC_GO@PP filter (blue line): (**a**) in the range 4000–500 cm^{-1}, (**b**) an enlargement of the region between 1600–500 cm^{-1}.

In both cases (untreated and UV treated), the filters s-PBC@PP and s-PBC_GO@PP show a wide band at 3700–3000 cm^{-1} due to the stretching vibrations of the hydroxyl group (OH group) from the water absorbed. This band is absent in the spectrum of the PP filter (black line), indicating its totally hydrophobic behavior. The features between 2800 cm^{-1}–3000 cm^{-1} are correlated with the asymmetric and symmetric CH stretching vibrations of the methyl groups. The band at around 1707 cm^{-1} is related to the C=O stretching vibrations (carboxylic groups). The band overlaps with the peak at 1645 cm^{-1} was also related to water. The presence of these signals confirms the greater hydrophilic character of the coated filters [29]. The region between 2400 cm^{-1} and 2000 cm^{-1} was discarded in the present study, being strongly influenced by the presence of carbon dioxide.

The peaks at 1411 cm^{-1}, 1126 cm^{-1}, 1035 cm^{-1} and 1006 cm^{-1} are due to SO_3^- (characteristic peaks), whereas the peak at 1151 cm^{-1} is related to the C-O stretching [36,37]. After UV treatment, the formation of new peaks was not visible. This indicates that the process did not induce structural changes in the polymer [38]. The FT-IR spectrum of GO shows characteristic peaks of carbonyl C=O at 1730 cm^{-1}, carboxyl C–O at 1410 cm^{-1}, as well as epoxy C–O at 1223 cm^{-1} [39]. However, these peaks overlap with the polymer peaks and, therefore, no appreciable variations between the IR spectra of the samples s-PBC@PP and s-PBC_GO@PP were observed.

The IR analysis confirms that the structure of s-PBC remained unaltered, also after dissolution in a polar solvent with or without GO flakes, and the coating layers are more hydrophilic than the PP itself.

3.1. s-PBC/s-PBC_GO Coatings for Co^{2+} Ions Removal

The Co^{2+} ions removal properties of s-PBC and a s-PBC_GO coated PP filters were explored using adsorption and filtration experiments. The source of the Co^{2+} ions used in this work was anhydrous $CoCl_2$, showing a blue color due to the chloride ions present in a tetrahedral arrangement around the Co^{2+} ion. When the salt is dissolved in water, the

strong solvation of Co^{2+} by water makes it difficult to maintain the tetrahedral complex in an aqueous solution and the hexaaqua complex ($[Co(H_2O)_6]^{2+}$), consisting of a Co^{2+} ion surrounded by six water molecules in an octahedral arrangement, is formed. The solution displays a pink color and its absorption band is found at 520 nm–525 nm [40].

Figure 3 reports the UV–VIS absorbance spectra of the $CoCl_2$ solutions, for the s-PBC@PP and s-PBC_GO@PP samples, untreated (Figure 3a) and UV treated (Figure 3b). The label inside Figure 3a also applies to Figure 3b. As shown in a previous work [33], even if the UV treatment does not produce structural changes in the polymer, it nevertheless affects the hydrophilicity of the surface.

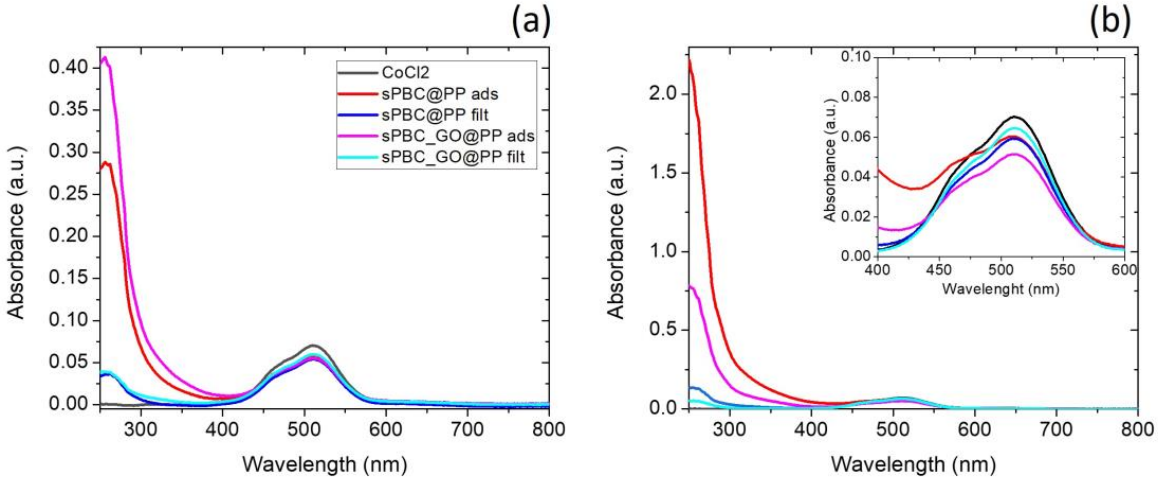

Figure 3. UV–Vis absorbance spectra of $CoCl_2$ solution for s-PBC@PP and s-PBC_GO@PP samples: (**a**) untreated and (**b**) UV treated. The label inside (**a**) also applies to (**b**). In (**b**) the spectrum of the $CoCl_2$ solution (black line) is covered by the other curves.

The UV–visible spectra showed a reduction in the absorbance peak at 520 nm for all the samples and processes as a result of cobalt ions removal and, simultaneously, an increase in the absorbance peak at 256 nm due to the release of by-products into each solution. This effect is enhanced for UV-treated samples after adsorption processes and this aspect is deeply discussed below considering the I_{250}/I_{515} ratio and Q_t values.

Table 1 reports the relative I_{250}/I_{515} ratio values and the Q_t as mg of the adsorbed ions on the gram of the coating layer, respectively, after filtration and adsorption processes for the s-PBC@PP and s-PBC_GO@PP samples, with or without UV treatment.

Table 1. Relative I_{250}/I_{515} ratio values and Q_t values for all the samples used in filtration and adsorption processes. The acronym "ads" or "filt" next to each filter name indicates the type of process (adsorption or filtration) in which the filter was involved.

Sample/Process	I_{250}/I_{515}	Q_t (mg/g)
s-PBC@PP/ads	4.81	21
s-PBC@PP/filt	0.65	24
s-PBC_GO@PP/ads	7.44	37
s-PBC_GO@PP/filt	0.60	21
s-PBC@PP UV/ads	34.84	20
s-PBC@PP UV/filt	2.50	17
s-PBC_GO@PP UV/ads	12.63	20
s-PBC_GO@PP UV/filt	0.87	13

The results for the uncoated PP filter are not reported because it does not show any removal activity. Coating the filter surface with a layer of s-PBC or s-PBC_GO makes the adsorption of Co^{2+} ions possible, thanks to the negatively charged groups. In addition to the sulphonic groups in the polymeric matrix, additional negatively charged oxygen

moieties are present when GO is added to s-PBC. The larger number of negative sites allows the higher adsorption capacity shown by the s-PBC_GO composite with respect to s-PBC itself to be explained (i.e., 37 mg/g and 21 mg/g, respectively). The main adsorption happened in the first 30 min, and afterwards just small variations occurred until they reached an equilibrium after two hours. Thus, Table 1 reports the values obtained for $CoCl_2$ adsorption after two hours of contact with the filters.

For the filtration processes, s-PBC showed a slightly higher removal efficiency with respect to adsorption, i.e., 24 mg/g, while the s-PBC_GO composite showed an even lower removal efficiency, i.e., 21 mg/g. If, on the one hand, the dispersion of GO flakes increases the number of active sites interacting with the metal ion, as observed by the adsorption efficiency, on the other hand, no evident effect on the filtration efficiency was observed after adding GO flakes inside the coating layer. The main difference was observed when comparing s-PBC_GO@PP adsorption or filtration: in the former, the interaction time between the Co ions and the active sites was higher than during filtration resulting in higher removal efficiency.

These results point out that the increase in the active adsorption site through the dispersion of GO flakes inside the polymeric matrix results in higher adsorption efficiency, but this is not sufficient to increase the filtration efficiency that strongly depends on the structure of the coating layer and the distribution of the GO flakes inside the polymeric layer.

The UV treatment does not seem to have any relevant effect as regards the adsorption processes for the s-PBC@PP filter, while a slight reduction in the efficiency was reported for the filtration. However, more negative effects on the adsorption and filtration processes were observed for the s-PBC_GO@PP filter, where a reduction in the Q_t was evident. This will be explained later in the text.

For all the samples used in the tests (adsorption and filtration), a significant variation in the absorbance spectra took place at wavelengths below 400 nm after the interaction of all the filters with the Co^{2+} ions solution, with the formation of a peak at 250 nm. The ratio values between the intensity of the peak at 250 nm and that at 515 nm, for all the filters and processes, are also reported in Table 1.

The data show that the intensity of I_{250}/I_{515} was higher in the case of adsorption than for the filtration processes for all the materials. Considering that the filtration processes last a few minutes, while the adsorption processes last two hours, it is clear that the longer the $CoCl_2$ interacts with the filter, the higher the I_{250}/I_{515} ratio. The presence of GO had the opposite effect on the I_{250}/I_{515} ratio, depending on the presence of UV treatment. For untreated samples, GO dispersion increased the Co^{2+} adsorption and also the I_{250}/I_{515} ratio. For UV-treated samples, even if the s-PBC and s-PBC_GO@PP samples have the same adsorption efficiency, the I_{250}/I_{515} ratio was lower for the sample with GO flakes.

We believe that the increase in the absorption peak at 250 nm depends on the interaction of cobalt with the sulfonic groups present in the polymer, and that this interaction leads to the formation and release of by-products. Indeed, sulfite ions were recently found to react with transition metals, such as Co and Fe, to generate oxysulfur radicals such as SO_4-, SO_3- and SO_5- used in the advanced oxidation process for water purification [41]. The sulfite ions have an absorption peak in the lower UV region of the UV–Vis absorbance spectrum, corresponding to the absorbance at 250 nm observed in our spectra. Our hypothesis is that the interaction of sulfonilic groups in the polymer with cobalt ions formed oxysulfur radicals within the release of sulfite ions in the solution (i.e., 250 nm absorbance peak) [41]. In the adsorption process, the interaction time between sulfonilic groups and Co ions is higher with respect to filtration, generating a larger amount of oxysulfur species in solution.

Furthermore, the I_{250}/I_{515} ratio increases for UV-treated samples. In particular, the absorbance spectrum of sample s-PBC@PP UV shows the greatest I_{250}/I_{515} ratio (34.84) after an adsorption process of two hours (Figure 3b, red line). The high value of the I_{250}/I_{515} ratio reported for UV-treated samples suggests that the formation of these new species in solution could be influenced by the presence of an electrical charge induced on the

coating surface. It was reported that, as an effect of such a modification, methylene blue (MB) in contact with the s-PBC polymer surface was transformed (in solution or when adsorbed on the polymer surface) into leuco form because of a reduction process involving the MB molecules. It was attributed to the presence of a negative charge induced on the polymer surface by UV irradiation [33]. Similarly, we think that an excess of electrons on the surface of the coated filters induced by UV treatment favors the formation of oxysulfur species in solutions due to the interaction with cobalt ions. For the samples treated with UV, although the absorption of the s-PBC_GO@PP UV sample was the same as the s-PBC@PP UV sample (Q_t = 20 mg/g), the I_{250}/I_{515} ratio was lower in the presence of GO (12.63 instead of 34.84). However, it is known that GO works as an electron scavenger when it is suitably coupled with other materials [42,43]. It is, therefore, possible that in the presence of a higher concentration of electrons (induced by the UV treatment), these are captured by the GO layers, thus, favoring the adsorption process of the ionic species (Co^{2+}) in the filter rather than its reaction with sulfonilic groups on the polymeric layers, followed by its release in solution.

For samples s-PBC@PP UV and s-PBC_GO@PP UV, five successive filtrations of the same aliquot of solution were conducted (not reported here). In both cases, the greatest reduction in Co ions occurs during the first filtration. The adsorption/filtration of these ions during the successive filtrations is quite negligible. However, the intensity of I_{250}/I_{515} continues to increase with the number of filtrations, as reported in Table 2.

Table 2. List of the processes and the I_{250}/I_{515} ratio for samples s-PBC@PP UV and s-PBC_GO@PP UV.

Process	s-PBC@PP UV	s-PBC_GO@PP UV
1st filtration	2.26	0.80
2nd filtration	3.59	1.19
3rd filtration	4.29	1.55
4th filtration	4.71	1.86
5th filtration	5.02	2.13

The trend in these values for both filters confirms that the Co^{2+} ions trapped on the filters continue to react with the sulfonic groups on the polymer in the presence of an excess of electrons and, then, oxysulfur species are released into the solution.

In order to investigate the induced modifications on the coating layers, the FT-IR and EDX spectra were acquired for the samples after interaction with the Co ion, in particular after the adsorption process since these report the higher I_{250}/I_{515} ratio values. Figure 4 reports the FT-IR spectra for: (a) s-PBC@PP UV and (b) s-PBC_GO@PP UV samples in the range 2000–500 cm^{-1}, before (black line) and after (red line) the Co^{2+} ion adsorption process.

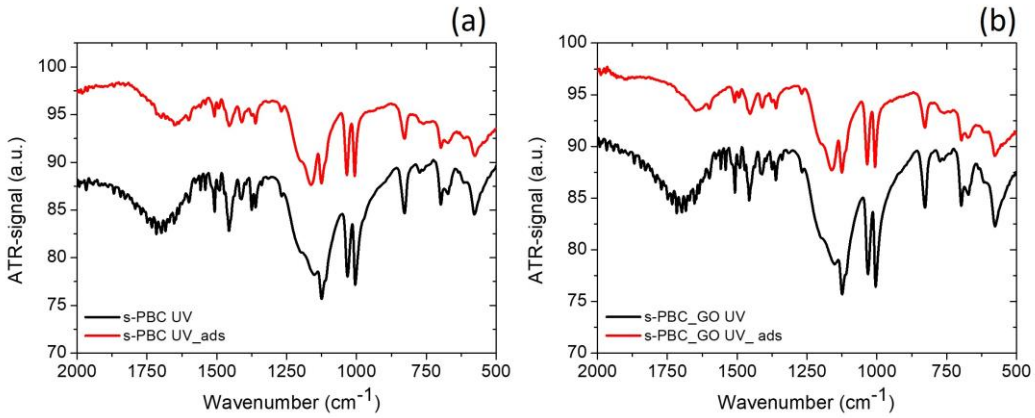

Figure 4. FT-IR spectra of: (**a**) s-PBC@PP UV filter and (**b**) s-PBC_GO@PP UV filter in the range 2000–500 cm^{-1}, before (black line) and after (red line) the Co^{2+} ion adsorption.

Comparing the spectra acquired for the samples before and after the adsorption of $CoCl_2$, the intensity of the S=O bonds reduces; the peaks related to C=O (1707 cm^{-1}) and C-O (1153 cm^{-1}) stretching shift to a lower and to a higher value, respectively. The presence of a shift is related to a variation in the electronic distribution in the bonds of the molecule. This redistribution could depend on a strong interaction between the polymer and the cationic species. Furthermore, the decrease in the S=O bonds (1411 cm^{-1}, 1126 cm^{-1}, 1035 cm^{-1} and 1006 cm^{-1}) is in line with the generation of oxysulfur species in solution after contact with the Co ions.

Figure 5 shows the carbon/oxygen (C/O), sulfur/oxygen (S/O) and sulfur/carbon (S/C) weight ratios obtained through the acquisition of EDX maps performed on the s-PBC@PP and s-PBC_GO@PP samples (untreated and UV treated), before and after immersion for 180 min in $CoCl_2$ solution.

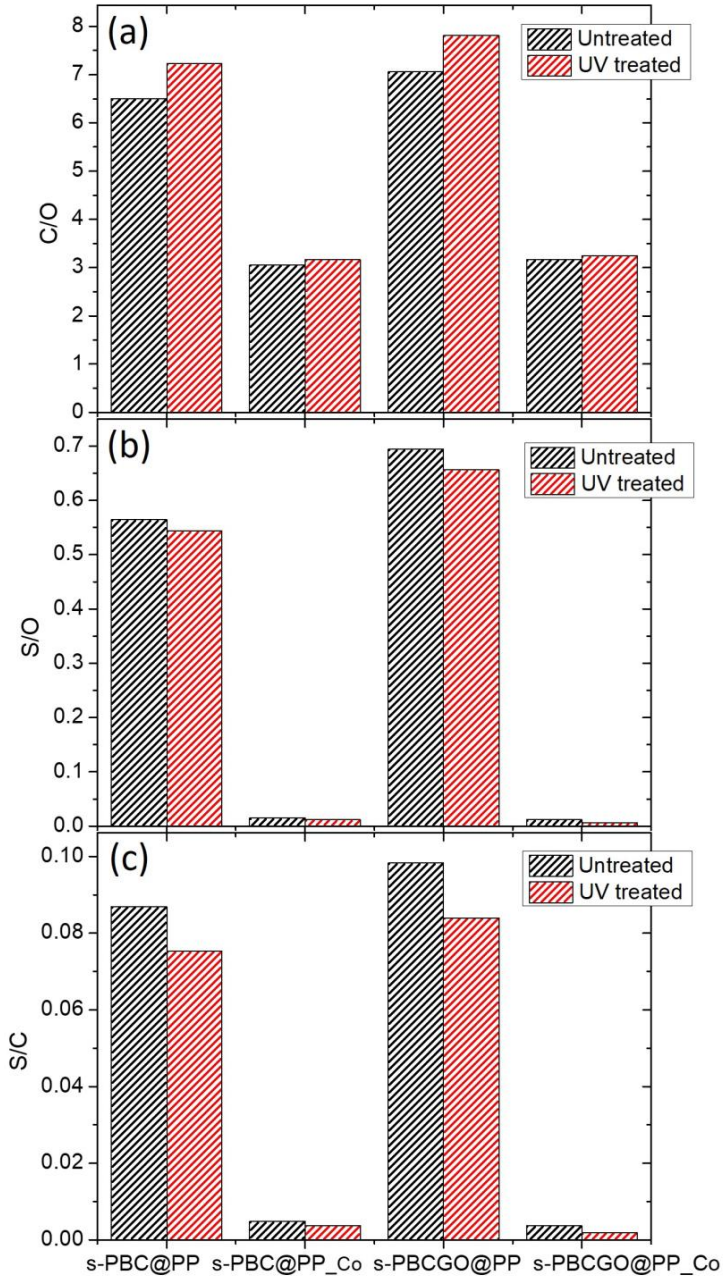

Figure 5. (**a**) C/O, (**b**) S/O and (**c**) S/C weight ratios obtained by EDX analysis carried out on s-PBC@PP and s-PBC_GO@PP (untreated and UV treated) samples, before and after being dipped for 180 min in a 17.5 mM $CoCl_2$ solution.

For samples treated with $CoCl_2$, the C/O, S/O and S/C weight ratios are strongly reduced compared to samples not exposed to the contaminant. UV treatment (red bars) only slightly modifies (reduces) the relative quantities of O and S compared to C, as it weakens the S=O bonds which are more susceptible to breaking. The high decrease in the S content in the samples after the interaction with $CoCl_2$ is in agreement with the FT-IR results (reported in Figure 4) that show a reduction in the S=O contributions (1411 cm^{-1}, 1126 cm^{-1}, 1035 cm^{-1} and 1006 cm^{-1}). The FT-IR and EDX analyses, thus, confirm that in the presence of the interaction between the cobalt ions and the polymer (in particular with the sulfonilic groups) oxysulfur species form and are released in solution from the polymeric layer.

Sulfate radical ($SO_4^{\cdot -}$) is an emerging oxidative species for the degradation of contaminants in various environmental matrices [44]. The main advantages of sulfate radicals with respect to hydroxyl ones are [45]: (1) the oxidation potential of $SO_4^{\cdot -}$ (2.5–3.1 V vs. NHE) is higher than OH; (2 $SO_4^{\cdot -}$ reacts more selectively and efficiently via electron transfer with organic compounds, in particular aromatic ones, over a wide pH range of 2–8; (3) the half-life period of $SO_4^{\cdot -}$ is generally supposed to be 30–40 times that of OH, which enables $SO_4^{\cdot -}$ to have more stable mass transfer and better contact with target compounds.

Compared to the past [46], the production of $SO_4^{\cdot -}$ through the use of sulfite [47] increased production, lowered production costs and lowered the toxicity of the formation process.

In fact, $SO_4^{\cdot -}$ can be generated in homogeneous or heterogeneous systems via photolysis, thermolysis and radiolysis or via transition metal activation (Co, Fe, Ni etc.) of persulfate (S_2O_8 PS) and peroxymonosulfate (SO5 PMS) [41].

According to the mechanism reported above, the Co (II) forms the Co(II)-SO_3 and it is oxidized to the Co(III)-SO_3+ complex with dissolved oxygen. As a consequence of the redox reaction between this complex and sulfite anions, Co (III) is reduced to Co (II) and the $SO_3^{\cdot -}$ radical is formed. This underwent many reactions with dissolved oxygen generating other oxysulfur radicals, such as $SO_4^{\cdot -}$ and $SO_5^{\cdot -}$. In our case, the sulfur radicals were generated by contact by the cobalt ions with sulfite anions on the polymer, according to the following reactions:

$$2R\text{-}SO_3^{-} \text{ (on polymer)} + Co(II) \rightarrow 2R\text{-}SO_3^{-}\ Co(II) + O_2 \rightarrow 2R\text{-}SO_3^{+-}\ Co(III)$$
$$2R\text{-}SO_3^{+-}\ Co(III) + 2R\text{-}SO_3^{-} \rightarrow 2\ R^{-}\ SO_3^{-}\ Co(II) + 2SO_3^{\cdot -} + 2R^{\cdot}$$

The above mechanism points out that sulfonilic groups on the polymeric layer are removed by the interaction with Co(II) and released in solution. This is evidenced by the peak at 250 nm, observed in the UV–Vis spectra of the Co solution where the samples were immersed (see Figure 3). Furthermore, the IR and EDX spectra acquired for the samples used for the Co ions adsorption and filtration showed a decrease in the signals linked to the S content. This effect is more evident for samples treated by UV: light is adsorbed, generating electrons that weaken the bonds in the sulfonilic moieties favoring the formation of oxysulfur radicals.

To confirm that the oxysulfur radicals are generated by a direct interaction between the Co ions and the sulfonilic groups on the membrane, adsorption experiments were repeated for the s-PBC@PP filters in the presence of multiple contaminants.

3.2. s-PBC Coatings for Multiple Contaminants Removal

S-PBC@PP filters as deposited and after UV treatment were immersed in 5 mL of methyl orange dye (MO 10^{-5} M) solutions in the presence or absence of $CoCl_2$ (17.5 mM). In this experiment, only adsorption processes were investigated since the radical generation effect was more evident for adsorption than for filtration.

The process of adsorption/degradation of the anionic MO was shown to occur partially, only after a protonation induced by contact with the s-PBC surface [28]. In principle, due to electrostatic effects, we expect that MO could interact with Co ions, therefore reducing

any interaction between the Co ions and sulfonic groups. A lower interaction between the polymer and Co ions would reduce the generation of oxysulfur radicals in solution.

Figure 6a reports the absorbance spectra for the MO (orange spectrum), MO + $CoCl_2$ mixed solution (brown spectrum), MO after the immersion of the polymer membrane (blue spectrum, named as "MO(H^+)"), MO + $CoCl_2$ mixed solution after the immersion of the polymer membrane (light green spectrum, named as "MO + Co (H^+)") and $CoCl_2$ (magenta spectrum). The immersion time for the membranes in the solutions was 60 min. For convenience in the labels, $CoCl_2$ is indicated by Co.

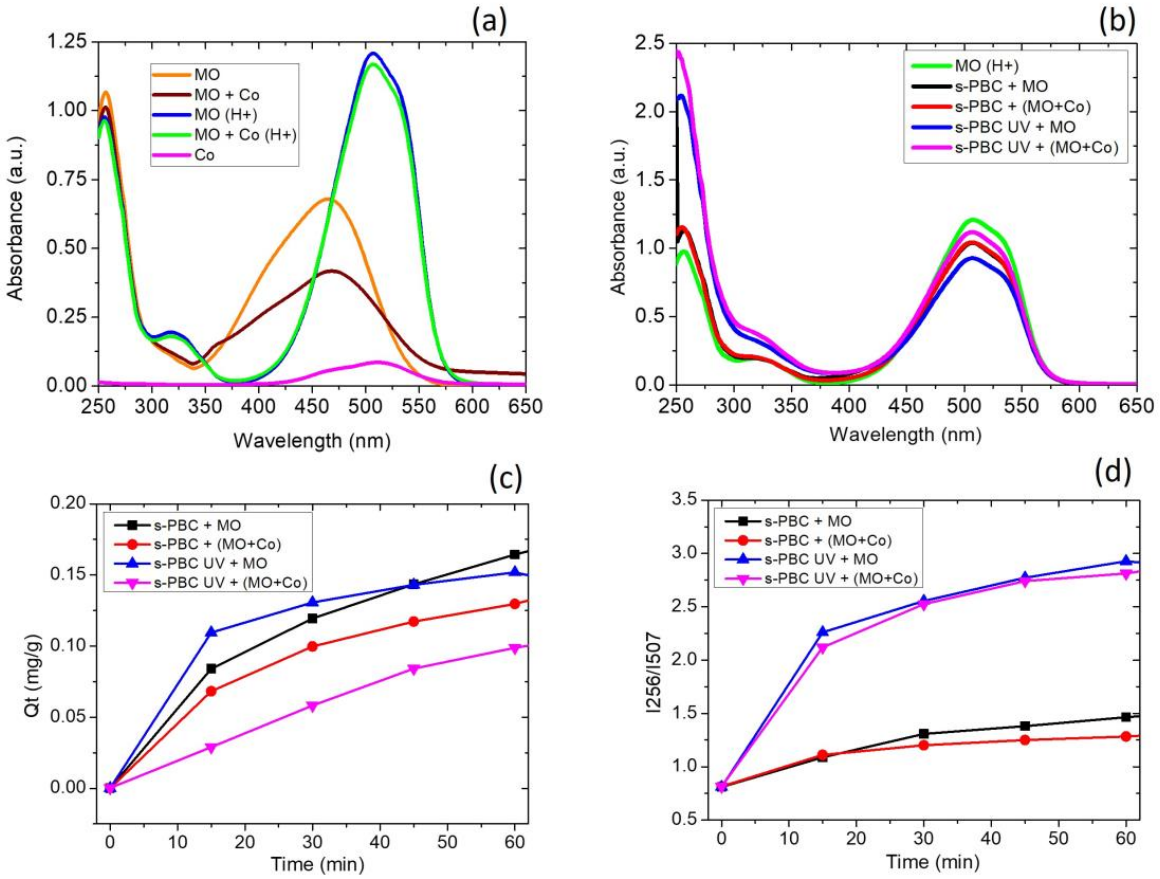

Figure 6. (**a**) Absorbance spectra for MO (orange spectrum), MO + Co mixed solution (brown spectrum), MO after the immersion of the polymer membrane (MO (H^+) (blue spectrum), MO + Co mixed solution after the immersion of the s-PBC membrane (MO + Co (H^+) (light green spectrum), $CoCl_2$ (Co, magenta spectrum). (**b**) Adsorption in the first 15 min for s-PBC@PP samples, with or without UV treatment, immersed in MO or MO + Co solutions. (**c**) Q_t versus adsorption time. (**d**) I_{256}/I_{507} ratio versus adsorption time.

The MO solution shows two bands, one at about 465 nm due to azo linkage and another at 257 nm due to benzene rings (orange spectrum). The $CoCl_2$ solution, instead, is characterized by an absorbance band at about 510 nm (magenta spectrum). In the mixed solution (MO + $CoCl_2$, brown spectrum), the Co ions and MO interact as evidenced by the decreasing and enlargement of the absorbance peak at 465 nm. By bringing the MO solution into contact with the polymeric samples, the solution immediately changes color, and the absorption spectrum changes (blue spectrum). The absorbance band at 465 nm shifts towards higher wavelengths (about 507 nm), a peak at 325 nm and an additional hump occurs at a larger wavelength on both peaks due to the protonation of MO. The same changes were observed for the MO + $CoCl_2$ solution put in contact with the s-PBC surface due to protonation of MO (blue spectrum), and the two spectra (green and blue) are superimposable. This means that in the presence of an acidic environment,

the interaction between the Co ions and MO (brown spectrum) is suppressed, the two species are distinguished in solution and the MO is protonated. Therefore, during the adsorption/degradation processes for the samples immersed in MO or MO + $CoCl_2$, the protonated MO spectrum was used as a reference spectrum (initial solution). For the calculation of the Q_t, the variation in the peak at 507 nm was considered.

As an example, Figure 6b shows the absorption in the first 15 min for the s-PBC@PP samples, with or without UV treatment, immersed in MO or MO + $CoCl_2$ solutions. The decision to show only these spectra depends on the fact that the most important changes occur after 15 min. All the samples show a reduction in the peak intensity at 507 nm. The peaks at 256 nm, instead, show small increases in the intensity for untreated samples, while a significant increase occurs for UV-treated samples. These trends will be used to explain the results reported in Figure 6c,d.

Figure 6c reports the Q_t versus the adsorption time, as mg of the adsorbed species of MO (peak at 507 nm) per gram of the s-PBC layer for the s-PBC@PP samples, with or without UV treatment. As shown in our previous work [28], MO adsorption onto s-PBC membranes is hindered, due to the electrostatic repulsions between the charge of the dye (negative) and the charge of sulfonilic groups (also negative). Only a few MO molecules are adsorbed, since these become positively charged due to their protonation.

Both for the untreated and the UV-treated samples, the Q_t is higher for the samples immersed in MO only and the greatest adsorption occurs in the first 15 min. This means that the MO adsorption (and therefore the removal) is hindered in the presence of Co ions, confirming a favored interaction by these ions with sulfonilic groups.

Figure 6d shows the I_{256}/I_{507} ratio versus the adsorption time. Also, in this case, after 15 min the maximum adsorption of the two species in solution takes place. The intensity of the peak at 507 nm depends only on the concentration of MO in solution, while the intensity of the peak at 256 nm depends both on the concentration of MO (it increases as the concentration decreases because the molecule breaks up and, therefore, the amount of benzene rings increases) and on the concentration of oxysulfur radicals released in solution (see Figure 3). Regarding the untreated samples (black curve and red curve), the two curves coincide in the first 15 min and then, the black curve has a slightly higher ratio (i.e., $I_{256} > I_{507}$). However, the Q_t value (Figure 6c) is higher for the s-PBC sample immersed in MO, with respect to the sample immersed in MO + $CoCl_2$. Anyway, the I_{256}/I_{507} ratio is the same at 15 min for both samples, confirming that the peak at 256 nm increased in the presence of Co and this increase is due to both MO degradation and oxysulfur radicals absorption at the same wavelength (256 nm).

For UV-treated samples (Figure 6c,d, blue and magenta lines), although MO removal is higher (higher Q_t) when no Co is present in solution, the I_{256}/I_{507} ratio is the same. Therefore, if the two values are equal, it means that in the case of the s-PBC sample in MO + $CoCl_2$ at 256 nm, besides the contribution related to MO degradation, there should be another one due to oxy-sulfuric groups, generated by the interaction of the Co ions with sulphonic groups on the polymer.

This effect is more evident in the presence of UV-treated samples, since the treatment introduces electrons on the polymer surface [33], which favor the formation of radical groups on the polymer surface and, therefore, the interaction with the cobalt.

4. Conclusions

In this work, polypropylene (PP) fibrous filters were coated with sulfonated pentablock copolymer (s-PBC) and s-PBC mixed with graphene oxide (s-PBC_GO). Some of them were treated with UV light to enhance their hydrophilicity. Tests for the removal of Co^{2+} ions from water by adsorption and filtration processes were carried out. In the filtration processes, the highest Q_t (24 mg/g) was shown by the s-PBC coated sample. Instead, for the adsorption processes, the highest Q_t (37 mg/g) was achieved by the s-PBC_GO coated sample. The dispersion of GO within the polymer seems to have a positive impact only for the adsorption properties, increasing the negative charge present on the coating surface

and favoring the adsorption of anionic compounds. No improvement is obtained with respect to the s-PBC as concerns the filtration efficiency.

During the adsorption processes, the interaction times between the ions and the filters are long, generating and releasing new species into solution (oxy-sulfuric radicals), as evidenced by the appearance of a new absorbance peak at 256 nm. Through FT-IR and EDX analysis it was possible to confirm the mechanisms involved in the metal ion removal processes. In particular, the interaction of cobalt ions with the sulfonic groups of the polymer were responsible for both the adsorption and the generation of oxysulfur radicals. In presence of another cationic contaminant, namely protonated MO, the interaction of the sulfur groups with Co is preferred, as evidenced by the formation of oxysulfur radicals. The mechanism of oxysulfur radicals formation was discussed and confirmed by studying the Co^{2+} ions adsorption experiments in the presence of a competitive organic contaminant (i.e., methyl orange, MO).

To conclude, the s-PBC layers, thanks to its hydrophilic, acidic and negatively charged character, gives additional functionalities to PP fibrous filters, that are just used as a support structure. The addition of GO is shown to increase the adsorption capabilities of the modified filter. However, in the presence of metal ions, the ion concentration and the ion/filter interaction time play a key role in the removal process and in the eventual formation of by-products. In this work, it was shown that the interaction between Co^{2+} ions and sulphonic groups in the polymer leads to the formation of unwanted secondary species (oxy-sulfur radicals). However, in the future, the generation of these oxidizing species could find applications in photocatalytic processes and for metals detection in water (sensing).

Author Contributions: Conceptualization, S.F., V.S. and S.S.; methodology, S.F., V.S. and S.S.; formal analysis, S.F., V.S. and S.S.; investigation, S.F., V.S., M.Z., S.L., L.L.P. and R.A.F.; resources, S.S.; data curation, S.F. and V.S.; writing—original draft preparation, S.F., V.S. and S.S.; writing—review and editing S.F., V.S., M.Z., S.L., L.L.P., R.A.F. and S.S.; visualization, S.F. and V.S.; supervision, S.S.; funding acquisition, S.S. All authors have read and agreed to the published version of the manuscript.

Funding: This work has been partially funded by the European Union (Next Generation EU), through the MUR-PNRR project SAMOTHRACE (ECS00000022).

Institutional Review Board Statement: Not applicable.

Informed Consent Statement: Not applicable.

Data Availability Statement: The data presented in this study are available on request from the corresponding authors.

Acknowledgments: The authors thank L. Gradon (Warsaw University of Technology) for providing PP fibrous filters and M. Italia (CNR-IMM) for technical support. Kraton LCC is acknowledged for providing the Nexar™ polymer.

Conflicts of Interest: The authors declare no conflict of interest.

References

1. Siddiqui, M.N.; Chanbasha, B.; Al-Arfaj, A.A.; Kon'kova, T.; Ali, I. Super-fast removal of cobalt metal ions in water using inexpensive mesoporous carbon obtained from industrial waste material. *Environ. Technol. Innov.* **2021**, *21*, 101257. [CrossRef]
2. Hussain, J.; Husain, I.; Arif, M.; Gupta, N. Studies on heavy metal contamination in Godavari River basin. *Appl. Water Sci.* **2017**, *7*, 4539–4548. [CrossRef]
3. Sayadi, M.H.; Rezaei, M.R.; Rezaei, A. Sediment Toxicity and Ecological Risk of Trace Metals from Streams Surrounding a Municipal Solid Waste Landfill. *Bull. Environ. Contam. Toxicol.* **2015**, *94*, 559–563. [CrossRef] [PubMed]
4. Alharbi, O.M.L.; Basheer, A.A.; Khattab, R.A.; Ali, I. Health and environmental effects of persistent organic pollutants. *J. Mol. Liq.* **2018**, *263*, 442–453. [CrossRef]
5. Sayadi, M.H.; Rezaei, M.R. Impact of land use on the distribution of toxic metals in surface soils in Birjand city. *Iran. Proc. Int. Acad. Ecol. Environ. Sci.* **2014**, *4*, 18–29.
6. Bernabé, I.; Gómez, B.J.M.; Díez, E.; Sáez, P.; Rodríguez, A. Optimization and adsorption-based recovery of cobalt using activated disordered mesoporous carbons. *Adv. Mate. Sci. Eng.* **2019**, *2019*, 3430176. [CrossRef]

7. Kara, M.; Yuzer, H.; Sabah, E.; Celik, M.S. Adsorption of cobalt from aqueous solutions onto sepiolite. *Water Res.* **2003**, *37*, 224–232. [CrossRef]
8. Zhong, Q.; Zhao, Y.Q.; Shen, L.; Hao, B.; Xu, X.; Gao, B.Y.; Shang, Y.N.; Chu, K.Z.; Zhang, X.H.; Yue, Q.Y. Single and binary competitive adsorption of cobalt and nickel onto novel magnetic composites derived from green macroalgae. *Environ. Eng. Sci.* **2020**, *37*, 188–200. [CrossRef]
9. Chenab, K.K.; Sohrabi, B.; Jafari, A.; Ramakrishna, S. Water treatment: Functional nanomaterials and applications from adsorption to photodegradation. *Mater. Today Chem.* **2020**, *16*, 100262. [CrossRef]
10. Wang, Z.; Wang, G.; Li, W.; Cui, Z.; Wu, J.; Akpinar, I.; Yu, L.; He, G.; Hu, J. Loofah activated carbon with hierarchical structures for high-efficiency adsorption of multi-level antibiotic pollutants. *Appl. Surf. Sci.* **2021**, *550*, 149313. [CrossRef]
11. Armaković, S.J.; Savanović, M.M.; Armaković, S. Titanium Dioxide as the Most Used Photocatalyst for Water Purification: An Overview. *Catalysts* **2023**, *13*, 26. [CrossRef]
12. Kumar, A.; Raizada, P.; Singh, P.; Saini, R.V.; Saini, A.K.; Hosseini-Bandegharaei, A. Perspective and status of polymeric graphitic carbon nitride-based Z-scheme photocatalytic systems for sustainable photocatalytic water purification. *Chem. Eng. J.* **2020**, *391*, 123496. [CrossRef]
13. Scuderi, V.; Impellizzeri, G.; Zimbone, M.; Sanz, R.; Di Mauro, A.; Buccheri, M.A.; Miritello, M.; Terrasi, A.; Rappazzo, G.; Nicotra, G.; et al. Rapid synthesis of photoactive hydrogenated TiO_2 nanoplumes. *Appl. Catal. B Env.* **2016**, *183*, 328–334. [CrossRef]
14. Wang, T.; Wu, H.; Zhao, S.; Zhang, W.; Tahir, M.; Wang, Z.; Wang, J. Interfacial polymerized and pore-variable covalent organic framework composite membrane for dye separation. *Chem. Eng. J.* **2020**, *384*, 123347. [CrossRef]
15. Guo, Y.; Liu, C.; Liu, H.; Zhang, J.; Li, H.; Zhang, C. Contemporary antibiofouling modifications of reverse osmosis membranes: State-of-the-art insights on mechanisms and strategies. *Chem. Eng. J.* **2022**, *429*, 132400. [CrossRef]
16. Zhao, D.L.; Zhao, Q.; Lin, H.; Chen, S.B.; Chung, T.-S. Pressure-assisted polydopamine modification of thin-film composite reverse osmosis membranes for enhanced desalination and antifouling performance. *Desalination* **2022**, *530*, 115671. [CrossRef]
17. Saleh, T.A.; Mustaqeem, M.; Khaled, M. Water treatment technologies in removing heavy metal ions from wastewater: A review. *Environ. Nanotechnol. Monit. Manag.* **2022**, *17*, 100617. [CrossRef]
18. Dotto, G.L.; McKayb, G. Current scenario and challenges in adsorption for water treatment. *J. Environ. Chem. Eng.* **2020**, *8*, 103988. [CrossRef]
19. Ali, I.; Gupta, V.K.; Aboul-Enein, H.Y. Metal ion speciation, and capillary electrophoresis: Application in the new millennium. *Electrophoresis* **2005**, *26*, 3988–4002. [CrossRef]
20. Ali, I.; Basheer, A.A.; Mbianda, X.Y.; Burakov, A.; Galunin, E.; Burakova, I.; Mkrtchyan, E.; Tkachev, A.; Grachev, V. Graphene-based adsorbents for remediation of noxious pollutants from wastewater. *Environ. Int.* **2019**, *127*, 160–180. [CrossRef]
21. Ali, I.; Alharbi, O.M.L.; Tkachev, A.; Galunin, E.; Burakov, A.; Grachev, V.A. Water treatment by new generation graphene materials: Hope for bright future. *Environ. Sci. Pollut. Res.* **2018**, *25*, 7315–7329. [CrossRef] [PubMed]
22. Zhang, T.; Xing, G.; Chen, W.; Chen, L. Porous organic polymers: A promising platform for efficient photocatalysis. *Mater. Chem. Front.* **2020**, *4*, 332–353. [CrossRef]
23. Wang, Y.; Yang, Z.; Liu, L.; Chen, Y. Construction of high performance thin-film nanocomposite nanofiltration membrane by incorporation of hydrophobic MOF-derived nanocages. *Appl. Surf. Sci.* **2021**, *570*, 151093. [CrossRef]
24. Bai, Y.; Gao, P.; Fang, R.; Cai, J.; Zhang, L.D.; He, Q.Y.; Zhou, Z.H.; Sun, S.P.; Cao, X.L. Constructing positively charged acid-resistant nanofiltration membranes via surface postgrafting for efficient removal of metal ions from electroplating rinse wastewater. *Sep. Purif. Technol.* **2022**, *297*, 121500. [CrossRef]
25. Giwa, A.; Ahmed, M.; Hasan, S.W. Polymers for Membrane Filtration in Water Purification. In *Polymeric Materials for Clean Water*; Springer: Berlin/Heidelberg, Germany, 2018; pp. 167–190.
26. Dmitrieva, E.S.; Anokhina, T.S.; Novitsky, E.G.; Volkov, V.V.; Borisov, I.L.; Volkov, A.V. Polymeric Membranes for Oil-Water Separation: A Review. *Polymers* **2022**, *14*, 980. [CrossRef]
27. Yu, T.; Zhou, J.; Liu, F.; Xu, B.M.; Pan, Y. Recent Progress of Adsorptive Ultrafiltration Membranes in Water Treatment—A Mini Review. *Membranes* **2022**, *12*, 519. [CrossRef]
28. Filice, S.; D'Angelo, D.; Scarangella, A.; Iannazzo, D.; Compagnini, G.; Scalese, S. Highly effective and reusable sulfonated pentablock copolymer nanocomposites for water purification applications. *RSC Adv.* **2017**, *7*, 45521–45534. [CrossRef]
29. Filice, S.; Mazurkiewicz-Pawlicka, M.; Malolepszy, A.; Stobinski, L.; Kwiatkowski, R.; Boczkowska, A.; Gradon, L.; Scalese, S. Sulfonated Pentablock Copolymer Membranes and Graphene Oxide Addition for Efficient Removal of Metal Ions from Water. *Nanomaterials* **2020**, *10*, 1157. [CrossRef]
30. D'Angelo, D.; Filice, S.; Scarangella, A.; Iannazzo, D.; Compagnini, G.; Scalese, S. Bi2O3/Nexar® polymer nanocomposite membranes for visible photocatalytic applications. *Catal. Today* **2019**, *321–322*, 158–163. [CrossRef]
31. Sciuto, E.L.; Filice, S.; Coniglio, M.A.; Faro, G.; Gradon, L.; Galati, C.; Spinella, N.; Libertino, S.; Scalese, S. Antimicrobial s-PBC Coatings for Innovative Multifunctional Water Filters. *Molecules* **2020**, *25*, 5196. [CrossRef]
32. Filice, S.; Sciuto, E.L.; Scalese, S.; Faro, G.; Libertino, S.; Corso, D.; Timpanaro, R.M.; Laganà, P.; Coniglio, M.A. Innovative Antibiofilm Smart Surface against Legionella for Water Systems. *Microorganisms* **2022**, *10*, 870. [CrossRef] [PubMed]
33. Filice, S.; Scuderi, V.; Libertino, S.; Zimbone, M.; Galati, C.; Spinella, N.; Gradon, L.; Falqui, L.; Scalese, S. Sulfonated Pentablock Copolymer Coating of Polypropylene Filters for Dye and Metal Ions Effective Removal by Integrated Adsorption and Filtration Process. *Int. J. Mol. Sci.* **2022**, *23*, 11777. [CrossRef] [PubMed]

34. Kujawska, A.; Kiełkowska, U.; Atisha, A.; Yanful, E.; Kujawski, W. Comparative analysis of separation methods used for the elimination of pharmaceuticals and personal care products (PPCPs) from water—A critical review. *Sep. Purif. Technol.* **2022**, *290*, 120797. [CrossRef]
35. Sikorska, E.; Gradoń, L. Biofouling reduction for improvement of depth Water filtration. *Filter production and testing. Chem. Process Eng.* **2016**, *37*, 319–330.
36. Dai, Z.; Ansaloni, L.; Ryan, J.J.; Spontak, R.J.; Deng, L. Incorporation of an ionic liquid into a midblock-sulfonated multiblock polymer for CO_2 capture. *J. Membr. Sci.* **2019**, *588*, 117193. [CrossRef]
37. Available online: https://www.sigmaaldrich.com/IT/it/technical-documents/technical-article/analytical-chemistry/photometry-and-reflectometry/ir-spectrum-table (accessed on 1 August 2023).
38. Chen, H.; Chang, K.; Men, X.; Sun, K.; Fang, X.; Ma, C.; Zhao, Y.; Yin, S.; Qin, W.; Wu, C. Covalent Patterning and Rapid Visualization of Latent Fingerprints with Photo-Cross-Linkable Semiconductor Polymer Dots. *ACS Appl. Mater. Interfaces* **2015**, *7*, 14477–14484. [CrossRef]
39. Guo, H.; Peng, M.; Zhu, Z.; Sun, L. Preparation of reduced graphene oxide by infrared irradiation induced photothermal reduction. *Nanoscale* **2013**, *5*, 9040. [CrossRef]
40. Dutta, D.; Dubey, R.; Dwivedi, S.K.; Puzari, A. Colorimetric Detection of Cobalt in Different Solvents by Using Their Solvatochromic Properties. *Saudi J. Eng. Technol.* **2020**, *5*, 144–149. [CrossRef]
41. Yuan, Y.; Zhao, D.; Li, J.; Wu, F.; Brigante, M.; Mailhot, G. Rapid oxidation of paracetamol by Cobalt(II) catalyzed sulfite at alkaline pH. *Catal. Today* **2018**, *313*, 155–160. [CrossRef]
42. Yeh, T.-F.; Cihlář, J.; Chang, C.-Y.; Cheng, C.; Teng, H. Roles of graphene oxide in photocatalytic water splitting. *Mater. Today* **2013**, *16*, 78–84. [CrossRef]
43. Liu, J.; Durstock, M.; Dai, L. Graphene oxide derivatives as hole- and electron-extraction layers for high-performance polymer solar cells. *Energy Environ. Sci.* **2014**, *7*, 1297–1306. [CrossRef]
44. Velo-Gala, I.; Farre, M.J.; Radjenovic, J.; Gernjak, W. N-Nitrosodimethylamine (NDMA) degradation by the ultraviolet/peroxodisulfate process. *Environ. Sci. Technol. Lett.* **2019**, *6*, 106–111. [CrossRef]
45. Hu, P.; Long, M. Cobalt-catalyzed sulfate radical-based advanced oxidation: A review on heterogeneous catalysts and applications. *Appl. Catal. B Environ.* **2016**, *181*, 103–117. [CrossRef]
46. Wacławek, S.; Lutze, H.V.; Grübel, K.; Padil, V.V.T.; Cerník, M.; Dionysiou, D.D. Chemistry of persulfates in water and wastewater treatment: A review. *Chem. Eng. J.* **2017**, *330*, 44–62. [CrossRef]
47. Luo, T.; Peng, Y.; Chen, L.; Li, J.; Wu, F.; Zhou, D. Metal-free electro-activated sulfite process for As(III) oxidation in water using graphite electrodes. *Environ. Sci. Technol.* **2020**, *54*, 10261–10269. [CrossRef]